
DIGITAL ACCESS TO SCHOLARSHIP AT HARVARD
DASH.HARVARD.EDU


HARVARD LIBRARY
Office for Scholarly Communication

Scattering of \(Yb\) and \(Yb^+\)

The Harvard community has made this article openly available. Please share how this access benefits you. Your story matters

Citation	Zhang, Peng, Alex Dalgarno, and Robin Cote. 2009. Scattering of Yb and Yb+. Physical Review A 80(3): 030703.
Published Version	doi:10.1103/PhysRevA.80.030703
Citable link	http://nrs.harvard.edu/urn-3:HUL.InstRepos:5140141
Terms of Use	This article was downloaded from Harvard University's DASH repository, and is made available under the terms and conditions applicable to Other Posted Material, as set forth at http://nrs.harvard.edu/urn-3:HUL.InstRepos:dash.current.terms-of-use#LAA

PHYSICAL REVIEW A **80**, 030703(R) (2009)

Scattering of Yb and Yb^+

Peng Zhang,[1] Alex Dalgarno,[1] and Robin Côté[2]
[1]*ITAMP, Harvard-Smithsonian Center for Astrophysics, Cambridge, Massachusetts 02138, USA*
[2]*Department of Physics, U-3046, University of Connecticut, Storrs, Connecticut 06269, USA*
(Received 10 July 2009; published 28 September 2009)

We calculate the cross sections for scattering of a neutral ytterbium atom with its positive ion at energies up to 30 eV. We identify peaks in the forward direction as arising from elastic collisions and those in the backward direction as from charge transfer. We show that the total cross section follows a semiclassical expression over a large range of energies and that the resonant charge transfer may be characterized by four energy regimes: an *s*-wave regime at ultralow energies, a modified Langevin regime at low energy, a Langevin regime at medium energy, and an "exchange" regime at high energy. We find large variations between the different isotopes for the two lowest-energy regimes and very little variation for the two highest-energy regimes. Our results are consistent with recent measurements.

DOI: 10.1103/PhysRevA.80.030703 PACS number(s): 34.70.+e, 31.15.ap, 31.50.−x

Over the last few years, there has been an increasing interest in studying ultracold systems that include atoms and ions. Ultracold atomic systems, in which electric charge play an important role, include ultracold plasmas [1–3], ultracold Rydberg gases [4,5], and ionization experiments in a Bose-Einstein condensate (BEC) [6,7]. Early studies of atom-ion collisions [8] showed that large elastic cross sections could occur and ions could be sympathetically cooled by neutral atoms, while resonant charge transfer could dominate charge transport at extremely low temperatures [9].

Experiments using hybrid traps have been proposed to cool ions with ultracold atoms, such as Ca^+ using Na [10], where the role of hyperfine interactions could also be explored [11], while other proposals suggest controlling collisions by movable trapping potentials [12]. Recently, an experiment involving a dual atom-ion trap for Yb [13] has been successful at measuring charge-transfer rates. Other experiments [14] are underway to detect large molecular ion clusters predicted to form when an ion is injected in a BEC [15]. Such ions have also been proposed for scanning tunneling microscopy of ultracold atoms [16] that could also be used to probe the ultracold Fermi atoms near quantum degeneracy [17].

Grier *et al.* [13] reported measurements of charge exchange in collisions of Yb^+ ions with neutral Yb atoms of a different isotopic composition.

$$^A\mathrm{Yb}^+ + {}^B\mathrm{Yb} \rightarrow {}^A\mathrm{Yb} + {}^B\mathrm{Yb}^+ + \Delta E, \qquad (1)$$

where the superscripts A and B label the isotopes. Because of the different isotope shifts of the ion and the neutral atom, there is a small energy difference ΔE. The rate coefficient k_{ch}^+ for the forward reaction and k_{ch}^- for the reverse reaction are related by $k_{\mathrm{ch}}^+ = k_{\mathrm{ch}}^- e^{-\Delta E/k_B T}$ [18]. Grier *et al.* found that in the range of kinetic energy E from 3×10^{-6} to 4×10^{-3} eV (corresponding to $T=E/k_B$ of 35 mK to 46.4 K), a factor of 1000, the rate coefficients for the isotope pairs with mass number 171, 172, and 174 are the same to within a factor of a few, and the rate coefficients k_{ch}^+ for the forward reaction of $^{174}\mathrm{Yb}^+$ and $^{172}\mathrm{Yb}$ are equal to those for the reverse reaction k_{ch}^-. The measurements suggest therefore that $\Delta E/E$ may be put equal to zero for $E\sim k_B T$ much above 3×10^{-6} eV (35 mK) in which case the process is reduced to resonance charge transfer.

Resonance scattering at low energies is determined by the lowest $^2\Sigma_g^+$ and $^2\Sigma_u^+$ Born-Oppenheimer states of the molecular ion Yb_2^+. We have carried out refined calculations of the corresponding interaction potentials, taking care to ensure that at large internuclear distance R they behave as $-\alpha_d/2R^4$ where α_d is the dipole polarizability of Yb. The interaction potentials $V_u(R)$ and $V_g(R)$, corresponding to the *gerade* state $^2\Sigma_g^+$ and *ungerade* state $^2\Sigma_u^+$, respectively, are presented in Fig. 1. They were calculated using the multireference average quadratic coupled-cluster method [19] combined with the relativistic small-core energy-adjusted pseudopotential [20]. By fitting them at large R, we derive $\alpha_d=144$ a.u., which agrees with direct calculations [21–23].

In resonant scattering of identical isotopes, $\Delta E=0$ and particles undergoing elastic scattering cannot be distinguished from particles undergoing charge exchange. However, with increasing energy, two distinct peaks develop in the angular distribution, one at forward scattering angles

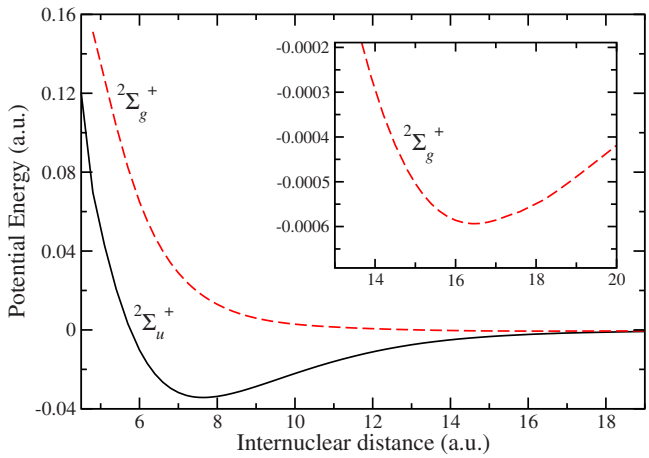

FIG. 1. (Color online) Potential energy curves of Yb_2^+ in atomic units (Hartree) as a function of the separation (in atomic units a_0: Bohr radius). The inset shows an enlargement of the shallow well of the $^2\Sigma_g^+$ state.

 ©2009 The American Physical Society

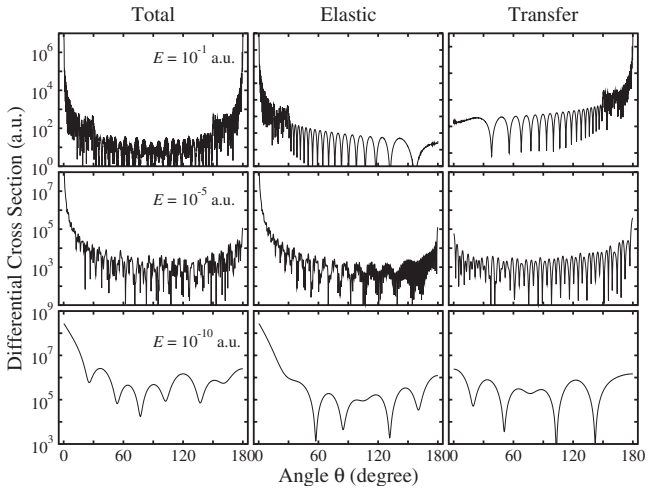

FIG. 2. Differential cross sections $I_{\rm tot}(\theta)$, $I_{\rm el}(\theta)$, and $I_{\rm ch}(\theta)$ of ^{172}Yb ion-atom collisions (with $s=0$) at high (top row), medium (middle row), and low (bottom row) energy. The cross sections are in atomic units (a_0^2) and the angles in degrees. The scattering peak at small angles corresponds to $I_{\rm el}(\theta)$. The peak at large angles, clearly due to charge transfer at higher energies, diminishes at lower energies, where $I_{\rm ch}$ still dominates but less noticeably.

($\theta\sim 0$) that can be empirically attributed to elastic scattering and the other at backward angles ($\theta\sim\pi$) that can be attributed to charge exchange.

The differential scattering cross section is given as a function of the scattering angle θ by the expression

$$I_{\rm tot}(\theta) = \frac{x}{4}|f^g(\theta) + f^g(\pi-\theta) + f^u(\theta) - f^u(\pi-\theta)|^2 + \frac{1-x}{4}|f^g(\theta) - f^g(\pi-\theta) + f^u(\theta) + f^u(\pi-\theta)|^2, \tag{2}$$

where x is given in terms of the total nuclear spin s by $x=(s+1)/(2s+1)$ for integer s and by $x=s/(2s+1)$ for half-integer s, and f^u and f^g are the scattering amplitudes corresponding respectively to the interaction potentials $V_u(R)$ and $V_g(R)$ of Yb_2^+ [24].

Figure 2 presents the calculated results of $I_{\rm tot}(\theta)$ for ^{172}Yb with $s=0$ ($s=0$ holds for the stable isotopes of mass number 168, 170, 172, 174, and 176) as a function of the collision energy. It illustrates the development of the scattering peaks near $\theta=0$ and $\theta=\pi$. There is little overlap of the scattering amplitudes at θ and $\pi-\theta$, and we may write for the total differential cross section

$$I_{\rm tot}(\theta) = I_{\rm el}(\theta) + I_{\rm ch}(\theta), \tag{3}$$

where

$$I_{\rm el}(\theta) = \frac{1}{4}|f^g(\theta) + f^u(\theta)|^2 \tag{4}$$

and

$$I_{\rm ch}(\theta) = \frac{1}{4}|f^g(\theta) - f^u(\theta)|^2. \tag{5}$$

$I_{\rm el}(\theta)$ describes the elastic scattering and $I_{\rm ch}(\theta)$ describes the charge exchange scattering. We note that neglecting cross terms like $f^g(\theta)f^u(\pi-\theta)$, etc., in Eq. (2) to obtain Eq. (3) removes the dependence on s in definitions (3)–(5). Figure 2 illustrates how the scattering peak at small angles ($\theta\sim 0$) corresponds to the elastic process (as expected classically), while charge transfer dominates the peak at large angles ($\theta\sim\pi$) at higher energies. However, as the collision energy diminishes, that domination becomes less striking. If we adopt the standard procedure and express f^u and f^g in terms of the phase shifts η_ℓ^g and η_ℓ^u, we obtain the cross sections for the total scattering

$$\sigma_{\rm tot} = \frac{2\pi}{k^2}\sum_{\ell=0}^{\infty}(2\ell+1)(\sin^2\eta_\ell^u + \sin^2\eta_\ell^g) \tag{6}$$

$$= \frac{1}{2}(\sigma_{\rm el}^g + \sigma_{\rm el}^u), \tag{7}$$

where $\sigma_{\rm el}^{g,u} \equiv \frac{4\pi}{k^2}\Sigma_{\ell=0}^{\infty}(2\ell+1)\sin^2\eta_\ell^{g,u}$ and charge exchange

$$\sigma_{\rm ch} = \frac{\pi}{k^2}\sum_{\ell=0}^{\infty}(2\ell+1)\sin^2(\eta_\ell^u - \eta_\ell^g). \tag{8}$$

Here, $k=\sqrt{2\mu E}/\hbar$ is the wave number and μ is the reduced mass. The elastic cross section can be defined from those two expressions: $\sigma_{\rm el}=\sigma_{\rm tot}-\sigma_{\rm ch}$.

The total cross section is dominated by the long-range R^{-4} potential. By using the random phase approximation [8,24] for low angular momenta and the semiclassical approximation for high angular momenta, the total cross section can be approximated by [8,25]

$$\sigma_{\rm tot}(E) = \pi\left(\frac{\mu\alpha_d^2}{\hbar^2}\right)^{1/3}\left(1+\frac{\pi^2}{16}\right)E^{-1/3}. \tag{9}$$

Figure 3 compares the cross sections for ^{172}Yb obtained by summing the individual contribution [Eq. (6)] with the approximate expression (9). The agreement is remarkably close even for energy as low as 3×10^{-9} eV ($\sim$35 μK). In the limit of zero energy, $\eta_0^{g,u}=-ka_{g,u}$, where a_g and a_u are the $^2\Sigma_g^+$ and $^2\Sigma_u^+$ scattering lengths, respectively, so that the total, charge exchange and elastic cross sections are equal to $2\pi(a_g^2+a_u^2)$, $\pi(a_g-a_u)^2$, and $\pi(a_g+a_u)^2$, respectively. We list the scattering lengths in Table I for the stable Yb isotopes. Scattering lengths are determined by the location of the least bound level and are very sensitive to the interaction potential and to the reduced mass. For heavy atoms and for an R^{-4} potential, they will, in general, tend to be large.

The resonant charge exchange cross sections of the stable isotopes are illustrated in Fig. 4 for energies up to 1 eV (10^4 K). Below 10^{-4} eV (1.16 K), the cross sections vary significantly from one isotope to another and they exhibit a pronounced oscillatory behavior which is more noticeable the smaller the zero energy cross section. The structure arises from a combination of shape resonances modulated by glory oscillations and Regge oscillations [26,27]. At eV energies,

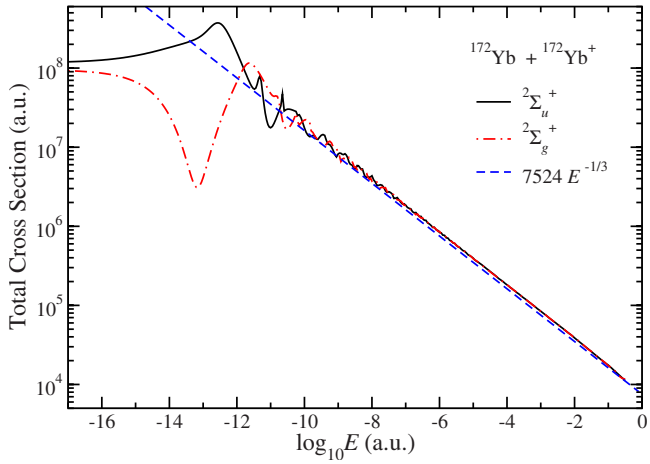

FIG. 3. (Color online) Total cross sections of ^{172}Yb ion-atom collisions in atomic units (a_0^2). We show the individual gerade and ungerade contributions and the semiclassical result with the prefactor of 7524 a.u. obtained from Eq. (9).

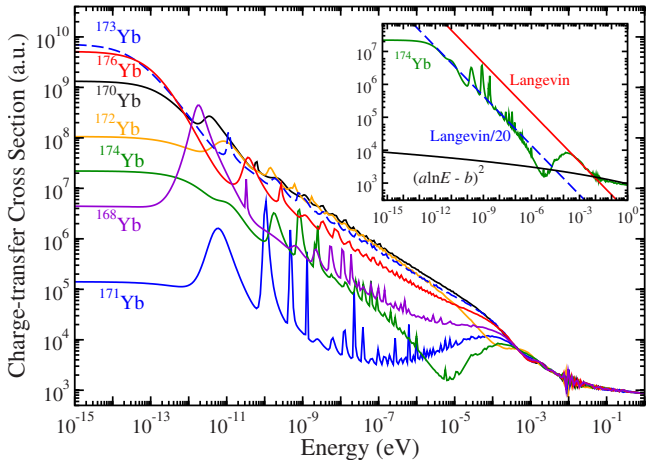

FIG. 4. (Color online) Charge-transfer cross sections of resonance ion-atom collisions for stable Yb isotopes. The inset reproduces the results for ^{174}Yb to illustrate the various energy regimes of σ_{ch}.

the cross sections vary as $(a \ln E - b)^2$ [24,25], a behavior that reflects the exponential decrease in the exchange energy at large R. For isotope 172, $a=1.88$ a.u. and $b=32.44$ a.u. with E measured in eV and σ_{ch} in units of a_0^2 (the values are comparable for the other isotopes). The resonant charge transfer exhibits four different energy regimes (see inset of Fig. 4): an s-wave regime at ultralow energies (described by the scattering lengths), a modified Langevin regime at low energy (where significant structure appears) which overall behave as $E^{-1/2}$, a Langevin regime at medium energy scaling as $E^{-1/2}$ [8], and an "exchange" regime [which follows $(a \ln E - b)^2$] at high energy. At much higher energy still (not shown on the figure), the cross section is expected to decrease as a high power of E (as E^{-6} for the Brinkman-Kramers cross section [28]).

Averaging over the velocity distribution suppresses the oscillatory structure. Figure 5 presents the thermal rate coefficients for several isotopes. They agree with each other to within a factor of a few until they enter the Wigner regime where the rate coefficients have constant values that are sensitive to the scattering lengths. At mean energies around 10^{-4} eV (1.16 K) the agreement with experiment [13] is encouraging and could be improved by a slight acceptable modification of the interaction potentials. With the exception of the two end points of the experimental energy range, the measurements cluster around a value of 6×10^{-10} cm^3 s^{-1} which corresponds to the Langevin rate coefficient for a polarizability of 143 ~ 144 a.u. [21–23]. The results shown in Fig. 5 are suggestive of new measurements with different isotopes.

In conclusion, we computed total and resonant charge-transfer cross sections between Yb and Yb$^+$ over a large range of energies. We gave the differential cross section and showed that the peak at forward scattering angles can be attributed to elastic scattering while the other at backward angles can be attributed to charge exchange. We also found that the total cross section is adequately approximated by a semiclassical expression over a wide range of energy and that resonant charge transfer can be described by five different energy regimes. The two lowest-energy regimes exhibit important variations between the different isotopes, while the three highest-energy regimes are almost identical. Finally, we compared our results with recent measurements and found them to be in good agreement. The variation in the theoretical rate with isotope mass number points to the need of new measurements with different isotope mixtures.

TABLE I. Scattering lengths (in atomic units a_0) for the gerade (a_g) and ungerade (a_u) state of the Yb stable isotopes.

	Isotope mass number						
	168	170	171	172	173	174	176
a_g	474	21477	2077	−2761	−43253	4453	−9715
a_u	−719	923	1866	3048	4608	7105	30815

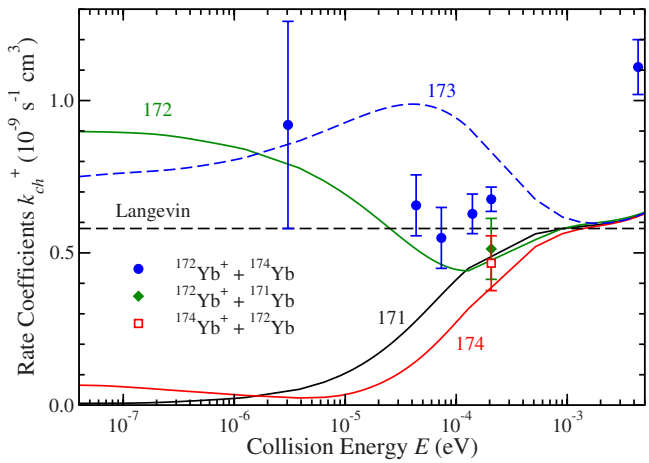

FIG. 5. (Color online) Thermal averaged charge-transfer rate of resonance ion-atom collisions of Yb+Yb$^+$ for various mass numbers. The experimental data of [13] and the Langevin value of 6×10^{-10} cm^3 s^{-1} are also shown.

The authors wish to thank A. T. Grier and V. Vuletić for helpful discussions. The research of A.D. and P.Z. was supported by the Chemical Science, Geoscience, and Bioscience Division of the Office of Basic Energy Science, Office of Science, (U.S.) Department of Energy and of R.C. was supported by the National Science Foundation.

[1] T. C. Killian, S. Kulin, S. D. Bergeson, L. A. Orozco, C. Orzel, and S. L. Rolston, Phys. Rev. Lett. **83**, 4776 (1999).
[2] S. Kulin, T. C. Killian, S. D. Bergeson, and S. L. Rolston, Phys. Rev. Lett. **85**, 318 (2000).
[3] T. C. Killian, M. J. Lim, S. Kulin, R. Dumke, S. D. Bergeson, and S. L. Rolston, Phys. Rev. Lett. **86**, 3759 (2001).
[4] W. R. Anderson, J. R. Veale, and T. F. Gallagher, Phys. Rev. Lett. **80**, 249 (1998).
[5] I. Mourachko, D. Comparat, F. de Tomasi, A. Fioretti, P. Nosbaum, V. M. Akulin, and P. Pillet, Phys. Rev. Lett. **80**, 253 (1998).
[6] D. Ciampini, M. Anderlini, J. H. Müller, F. Fuso, O. Morsch, J. W. Thomsen, and E. Arimondo, Phys. Rev. A **66**, 043409 (2002).
[7] M. Anderlini and E. Arimondo, e-print arXiv:physics/0505055.
[8] R. Côté and A. Dalgarno, Phys. Rev. A **62**, 012709 (2000).
[9] R. Côté, Phys. Rev. Lett. **85**, 5316 (2000).
[10] O. P. Makarov, R. Côté, H. Michels, and W. W. Smith, Phys. Rev. A **67**, 042705 (2003).
[11] Z. Idziaszek, T. Calarco, P. S. Julienne, and A. Simoni, Phys. Rev. A **79**, 010702(R) (2009).
[12] Z. Idziaszek, T. Calarco, and P. Zoller, Phys. Rev. A **76**, 033409 (2007).
[13] A. T. Grier, M. Cetina, F. Oručević, and V. Vuletić, Phys. Rev. Lett. **102**, 223201 (2009).
[14] J. H. Denschlag (private communication).
[15] R. Côté, V. Kharchenko, and M. D. Lukin, Phys. Rev. Lett. **89**, 093001 (2002).
[16] C. Kollath, M. Köhl, and T. Giamarchi, Phys. Rev. A **76**, 063602 (2007).
[17] Y. Sherkunov, B. Muzykantskii, N. d'Ambrumenil, and B. D. Simons, e-print arXiv:0802.3158.
[18] E. Bodo, P. Zhang, and A. Dalgarno, New J. Phys. **10**, 033024 (2008).
[19] P. G. Szalay and R. J. Bartlett, J. Chem. Phys. **103**, 3600 (1995).
[20] Y. Wang and M. Dolg, Theor. Chem. Acc. **100**, 124 (1998).
[21] P. Zhang and A. Dalgarno, J. Phys. Chem. A **111**, 12471 (2007).
[22] B. K. Sahoo and B. P. Das, Phys. Rev. A **77**, 062516 (2008).
[23] C. Thierfelder and P. Schwerdtfeger, Phys. Rev. A **79**, 032512 (2009).
[24] N. F. Mott and H. S. W. Massey, *The Theory of Atomic Collisions*, 3rd ed. (Oxford University Press, London, 1965).
[25] A. Dalgarno, Philos. Trans. R. Soc. London, Ser. A **250**, 426 (1958).
[26] P. S. Krstić, J. H. Macek, S. Y. Ovchinnikov, and D. R. Schultz, Phys. Rev. A **70**, 042711 (2004).
[27] J. H. Macek, P. S. Krstić, and S. Y. Ovchinnikov, Phys. Rev. Lett. **93**, 183203 (2004).
[28] R. Shakeshaft and L. Spruch, Rev. Mod. Phys. **51**, 369 (1979).